Journal of Steroid Biochemistry & Molecular Biology 125 (2011) 181–191

Contents lists available at ScienceDirect

Journal of Steroid Biochemistry and Molecular Biology

journal homepage: www.elsevier.com/locate/jsbmb

Cardiotonic steroids attenuate ERK phosphorylation and generate cell cycle arrest to block human hepatoma cell growth☆

Zhong-Wei Xu[a], Feng-Mei Wang[b], Mo-Jie Gao[a], Xiao-Yi Chen[a], Na-Na Shan[a], Shi-Xiang Cheng[a], Xia Mai[a], Ga-Hu Zala[a], Wen-Liang Hu[c], Rui-Cheng Xu[c,*]

[a] Department of Cell Biology, Medical College of the Chinese People's Armed Police Forces, Tianjin City 300162, China
[b] Tianjin 3rd Central Hospital, Tianjin City 300162, China
[c] Tianjin Key Laboratory for Biomarkers of Occupational and Environmental Hazards, Tianjin City 300162, China

ARTICLE INFO

Article history:
Received 10 August 2010
Received in revised form
28 December 2010
Accepted 30 December 2010

Keywords:
Ouabain
Cinobufagin
Na^+/K^+-ATPase
Hepatoma cancer
Apoptosis
Cell cycle

ABSTRACT

Recent studies revealed the potential of Na^+/K^+-ATPase as a target for anticancer therapy and showed additional modes of action of cardiotonic steroids (CSs), a diverse family of naturally derived compounds, as inhibitors of Na^+/K^+-ATPase. The results from epidemiological studies showed significantly lower mortality rates in cancer patients receiving CSs, which sparked interest in the anticancer properties of these drugs. The present study was designed to investigate the anticancer effect of CSs (ouabain or cinobufagin) and to elucidate the molecular mechanisms of CS activity in hepatoma cell lines (HepG2 and SMMC-7721). Ouabain and cinobufagin significantly inhibited cell proliferation by attenuating the phosphorylation of extracellular regulated kinase (ERK) and down-regulating the expression of C-myc. These CSs also induced cell apoptosis by increasing the concentration of intracellular free calcium ($[Ca^{2+}]_i$) and induced S phase cell cycle arrest by down-regulating the expression of Cyclin A, cyclin dependent kinase 2 (CDK2) and proliferating cell nuclear antigen (PCNA) as well as up-regulating the expression of cyclin dependent kinase inhibitor 1A ($p21^{CIP1}$). Overexpression of ERK reversed the antiproliferation effect of ouabain or cinobufagin in HepG2 and SMMC-7721 cells. Currently, the first generation of CS-based anticancer drugs (UNBS1450 and Anvirzel) are in Phase I clinical trials. These data clearly support their potential use as cancer therapies.

1. Introduction

Hepatocellular carcinoma (HCC) is the fifth most common cancer and the third leading cause of cancer death in the world. Only 10–20% of HCC patients can be treated surgically, while most HCC patients are treated exclusively with chemotherapy. However, treatment of HCC with a variety of anticancer agents, such as anthracene ring anticancer antibiotics, alkaloids, and the podophyllotoxin class of anticancer drugs is limited by multi-drug resistance (MDR). Research aimed at finding new targeted drugs for the treatment of HCC is therefore a high priority [1,2]. Cardiotonic steroids (CSs) are synthetic or naturally occurring steroid hormones extensively found in decorative plants or animal species, and they include ouabain, digoxin, cinobufagin and others. These compounds inhibit Na^+/K^+-ATPase activity by targeting the first 4–6 transmembrane regions of the Na^+/K^+-ATPase α subunit [3–6]. CSs have been widely used for the treatment of heart failure, but retrospective epidemiological studies revealed surprising results during the late 20th century: very few patients maintained on CS treatment for heart problems died from cancer, which suggested the possible use of these compounds in oncology [7,8]. Mijatovic found that the Na^+/K^+-ATPase *was* the Achilles heel of multi-drug-resistant cancer cells and showed that CSs could be especially applicable to notoriously drug-resistant cancers [9]. Anvirzel, which is an aqueous extract of the plant Nerium oleander, and UNBS1450, which is a semi-synthetic derivative of the novel cardenolide 2″-oxovoruscharin, have entered Phase I clinical trials and are showing more anticancer properties than platina derivatives, including cisplatin, carboplatin and oxaliplatin [10,11].

The properties of Na^+/K^+-ATPases identify this enzyme as a potential target for the development of anticancer drugs based on its role as a versatile signal transducer and the association of its overexpression and increased enzymatic activity with the development and progression of different cancers [12]. Prior studies reported that Na^+/K^+-ATPases are highly expressed in malignant cells, including human prostate cancer PC-3, DU-145 cells [11], human non-small cell lung cancer (NSCLC) A549 cells [13], glioblastoma Hs683, U373-MG, U87-MG, T98G cells [14], and breast cancer MCF-7 cells [15]. Mijatovic reported a significant reduction of cell

☆ Article from the special issue on steroids and cancer.

* Corresponding author.
E-mail address: xzw113@gmail.com (R.-C. Xu).

0960-0760/$ – see front matter © 2011 Elsevier Ltd. All rights reserved.
doi:10.1016/j.jsbmb.2010.12.016

invasion and proliferation caused by knock-down of Na^+/K^+-ATPase α1 subunit expression in (NSCLC) A549 cells [13]. The overexpression Na^+/K^+-ATPases in malignant cells might provide a higher number of target acceptors for CSs compared with normal cells to mediate the killing of tumour cells. However, the mechanisms mediating the anticancer effect of CSs in malignant cells remain unclear.

Previous studies have shown that inhibition of Na^+/K^+-ATPase activity by CSs causes an increase in intracellular Na^+ concentration, depolarisation of the cell membrane, activation of voltage-dependent Ca^{2+} channels and influx of extracellular [Ca^{2+}], resulting in an increase of intracellular [Ca^{2+}] that acted as a signal for apoptosis [16]. In addition to transporting ions, Na^+/K^+-ATPases interact with adjacent membrane proteins and trigger cytosolic cascades that send signals to intracellular organelles. The signalling pathways that were found to be rapidly elicited by the interaction of CSs with the Na^+/K^+-ATPase and that were independent of changes in intracellular Na^+ and K^+ concentrations include the deactivation of Src kinase [17], inhibition of the Src mediated activation of the epidermal growth factor receptor (EGFR) [18], and activation of IκB signalling [19].

The present study focused on the elucidation of the molecular mechanisms mediating the anticancer activity of CSs using ouabain and cinobufagin on human hepatoma cancer cell lines (HepG2 and SMMC-7721). CSs were found to inhibit cell proliferation by attenuating ERK phosphorylation, which correlated with the down-regulation of C-myc expression. These processes were hypothesised to induce cell apoptosis by increasing intracellular free Ca^{2+} concentration and to cause S phase cell cycle arrest by down-regulating the expression of Cyclin A, CDK2 and PCNA and up-regulating the expression of $p21^{CIP1}$. The present data also indicated that overexpression of ERK reversed the antiproliferation effect of ouabain or cinobufagin in HepG2 and SMMC-7721 cells. The current study provides experimental evidence and theoretical support for the development of CSs as novel anticancer therapeutic agents.

2. Materials and methods

2.1. Chemicals and reagents

Ouabain and cinobufagin were purchased from Sigma Aldrich (St. Louis, MO). H-DMEM medium and FBS were obtained from Gibco (NY, USA). Rabbit polyclonal anti ERK, and anti CDK2 antibodies, anti β-actin, mouse monoclonal anti-phospho-ERK, and goat anti-rabbit IgG-FITC were from Santa Cruz (Santa Cruz, CA). Mouse monoclonal anti C-myc, $P21^{CIP1}$ as well as rabbit polyclonal anti Cyclin A and PCNA antibodies were obtained from NeoMarkers (Fremont, CA). Anti-rabbit and anti-mouse IgG, horseradish peroxidase-linked secondary antibodies were purchased from KPL (Gaithersburg, MD). Enhanced chemiluminescence detection reagents were obtained from Amersham (USA). PrimeScript™ RT and all primers were from TaKaRa (Shiga, Japan), SYBR green PCR master mix was from ABI (Applied Biosystems, Foster, CA), Fura-3/AM was from Invitrogen (Invitrogen Carlsbad, CA), and Fura-2/AM was purchased from Sigma–Aldrich (St. Louis, MO).

2.2. Cell culture

Human hepatocellular carcinoma cell lines (HepG2, SMMC-7721) were obtained from ATCC (Manassas, VA) and routinely maintained in Dulbecco's modified Eagle's medium (DMEM) supplemented with 10% foetal bovine serum (GIBCO), 2 mmol/L L-glutamine (GIBCO) and 100 units/mL penicillin–streptomycin (GIBCO). All cultures were maintained at 37 °C in a humidified 5% CO_2 atmosphere and were mycoplasma-free. For flow cytometry of ouabain and cinobufagin treated cells, cells were washed in sterile PBS and cultured in serum free medium for at least 24 h prior to the addition of drugs.

2.3. Cell growth assay

Experiments were conducted in 96-well plates containing DMEM supplemented with 10% FBS. HepG2 and SMMC-7721 cells were seeded at a density of 4×10^3 cells/well in 200 μL of medium and cultured for 24 h. The medium was replaced with fresh complete medium, containing 10% FBS and different concentrations of ouabain (0.001, 0.01, 0.1, 1 and 10 μmol/L) and cinobufagin (0.01, 0.1, 1, 10, 10 and 100 μmol/L). A volume of 20 μL of CCK-8 reagent was added into each well at 24, 48 and 72 h. The plates were returned to the incubator for 3 h, and the absorbance at 450 nm was measured using an enzyme-linked immunosorbent assay microplate reader (Molecular Devices, Sunnyvale, USA). Cell growth was calculated using the following equation: % cell growth = $100[(O.D._{treatment} - O.D._{blank})/(O.D._{control} - O.D._{blank})]$. The drug concentrations required to inhibit cell growth by 50% (IC_{50}) were calculated from the cytotoxicity curves (Bliss's software; Bliss Co, CA, USA). IC_{50} = concentration of ouabain or cinobufagin resulting in 50% inhibition of cell growth. Values were expressed as means ± SD of three separate experiments.

2.4. Cell cycle analysis

A total of 5×10^5 cells were incubated at 37 °C overnight in 10-cm plastic dishes in DMEM supplemented with 10% FBS. Cells were cultured in serum free DMEM medium for 24 h and treated with various concentrations of ouabain (0, 0.1, 0.5 μmol/L) and cinobufagin (0, 1, 5 μmol/L) for 24 h. Cells were trypsinised, washed in cold phosphate-buffered saline (PBS, pH 7.4), fixed in 70% ethanol/30% PBS and stored at 4 °C until processing. A portion (1 mL) of the fixed cell suspension containing 1×10^6 cells was washed twice in cold PBS. The fixed cells were treated for 30 min at 4 °C in the dark with fluorochrome DNA staining solution (1 mL) containing 40 μg of propidium iodide (PI) and 0.1 mg of RNase A. Sub G_0/G_1, S, and G_2/M cells were gated out as appropriate. PI fluorescence was measured in the FL3 channel (670 nm long pass filter) after cell doublets were excluded by pulse processing. A total of 10,000 cells were counted per sample. Cell debris was excluded from the analysis by appropriately raising the forward scatter threshold. The data were analysed with CellQuest software.

2.5. Assessment of apoptosis by Hoechst staining

Hoechst 33342 staining was performed as follows. Cells were seeded in a 6-well chamber slide at a density of 5×10^4 cells/well and cultured for 24 h. Cell were then subjected to different treatments [0.5 μmol/L ouabain, 5 μmol/L cinobufagin, 2 mmol/L EGTA, 2 mmol/L EGTA + 0.5 μmol/L ouabain, 2 mmol/L EGTA + 5 μmol/L cinobufagin] for 24 h at 37 °C. Cells were fixed with ice-cold methanol:acetic acid (3:1) at room temperature for 10 min followed by two washes with ice-cold PBS and incubated with 10 μg/mL Hoechst 33342 for an additional 10 min. The changes in the nuclei of cells after Hoechst 33342 staining were observed under a fluorescent microscope (Olympus, BX-60, Japan).

2.6. $[Ca^{2+}]_i$ concentration measurement by confocal microscopy and spectrofluorophotometer

Cells were cultured on confocal culture dishes to approximately 70% confluence and treated with 0.5 μmol/L ouabain and 5 μmol/L cinobufagin for 24 h. The fluorescence indicator Fura-3/AM (Invitrogen, USA) was reconstituted in dimethylsulfoxide (DMSO) and

added to the samples at a final concentration of 10 μg/mL. The final concentration of DMSO in each sample was less than 0.1%. Cells were incubated in the dark for 60 min at 37 °C followed by a 30-min wash in Krebs buffer; fluorescence images were captured using a confocal microscope (FV500, Olympus, Japan). The excitation wavelength was 488 nm, and the emission wavelength was 510 nm. The fluorescence intensity was assessed by Image-Pro Plus 6.0 software.

To measure $[Ca^{2+}]_i$ by dual-wavelength spectrofluorophotometer, as described previously [20]. Cells were cultured on culture dishes to approximately 70% confluence and treated with 0.1, 0.5 μmol/L ouabain and 1, 5 μmol/L cinobufagin for 24 h. The fluorescence indicator Fura-2/AM (Sigma, Dorset, UK) was dissolved in dimethylsulfoxide and aliquots (10 μL) were stored at −20 °C until used. Cell suspensions were incubated with 3 μmol/L of fura-2/AM in 3 mL for 30 min for 37 °C in the dark. A standard intracellular calibration procedure was performed after cell permeabilisation with 5 μmol/L ionomycin (Sigma) to calculate the $[Ca^{2+}]_i$ from the ratio of the fluorescence intensities emitted at the two wavelengths and measured by spectrofluorophotometer (RF-5301PC) (Shimadzu, Japan). The Grynkiewicz equation was used, providing a dissociation constant of 225 nmol/L of fura-2/AM for Ca^{2+}. The R_{min} value was obtained by perfusing permeabilised cells with Krebs buffer in which $CaCl_2$ was replaced by 2 mmol/L EGTA. The Grynkiewicz equation is as follows: $[Ca^{2+}]_i$ (nmol/L) = $K_d \times [(R - R_{min})/R_{max} - R)] \times$ Sfb, where the Kd for Ca^{2+} binding to fura-2/AM at 37 °C = 225 nmol/L, R = 340/380 ratio, R_{max} = 340/380 ratio under Ca^{2+}-saturating condition, R_{min} = 340/380 ratio under Ca^{2+}-free conditions, and Sfb = ratio of baseline fluorescence (380 nm) under Ca^{2+}-free and -bound conditions. The R_{max}, R_{min}, and the derived Sfb along with measured R values from cell suspensions were substituted into the Grynkiewicz equation and $[Ca^{2+}]_i$ was estimated.

2.7. RNA isolation and reverse transcription real-time PCR

Cells were seeded into 6-cm plastic dishes at a density of 5×10^5 cells/dish and cultured for 24 h. Subsequently, 0.1 and 0.5 μmol/L ouabain and 1 and 5 μmol/L cinobufagin were added. After 24 h, total RNA was isolated using the TRIzol reagent (Invitrogen, Carlsbad, CA) according to the manufacturer's protocol. First-strand cDNA samples were synthesised using a TaqDNA polymerase (TaKaRa Shiga, Japan). For real-time PCR quantification, β-actin RNA levels were quantified in all samples as an internal control. Messenger RNA (mRNA) levels were calculated relative to β-actin mRNA. Real-time PCR was performed in a 25-μl volume with SYBR Green PCR Master Mix (Applied Biosystems, CA). Fluorescence was detected on an ABI 7500 system (Applied Biosystems, CA). Primer sequences for real-time PCR were as follows: ERK: 5′-TACACCAACCTCTCGTACATCG-3′ (forward) and 5′-CATGTCTGAAGCGCAGTAA GATT-3′ (reverse); C-myc: 5′-TGGTCGCCCTCCTATGTTG-3′ and 5′-CCGGGTCGCAGATGAAACTC-3′; PCNA: 5′-GGCTCCATCCTCAAGAAGGTG-3′ and 5′-GGGACGAGTCCATGCTCTG-3′; cyclin A: 5′-CGCTGGCGGTACTGAAGTC-3′ and 5′-AAGGAGGAACGGTGACATGC-3′; CDk2: 5′-ACCTCCAGGAGATTCCAGACC-3′ and 5′-CCCAGGTTTGAGAGCAGTTCC-3′; $P21^{CIP1}$: 5′-CCTGTCACTGTCTTGTACCCT-3′ and 5′-CCCGCAGTATCTTGCCTCC-3′; β-actin: 5′-CTAGGGTGCAAGCCCAAGGA-3′ and 5′-ACAGTT ATGCCAAGCCCACCA-3′. Sample mRNAs were normalised to the respective β-actin expression levels. The results were expressed as fold induction.

2.8. Western blot analysis

Cells were seeded on culture dishes and grown to 85% confluence, cultured in 0.1 and 0.5 μmol/L ouabain and 1 and 5 μmol/L cinobufagin for 24 h, lysed in lysis buffer (50 mmol/L Tris–HCl, pH 7.4, 150 mmol/L NaCl, 1 mmol/L EDTA, 5% (v/v) β-mercaptoethanol, 1% Nonidet P-40, 0.25% sodiodeoxycholate, 5 μg/mL leupeptin, 5 μg/mL aprotinin, 0.2 mmol/L phenylmethyl sulfonyl fluoride) and incubated on ice for 30 min, followed by centrifugation at 14,000 rpm for 20 min. The supernatant was stored at −70 °C. Protein concentrations were measured with the BCA protein assay (Pierce, Rockford, IL), and samples were diluted to obtain equal concentrations. A total of 60 μg of total protein lysate for each sample was diluted in reducing sample buffer and subjected to 12% SDS-PAGE in 1 × TGS (Tris–glycine SDS) at 100 V for 2 h. The proteins were then electrotransferred to polyvinylidene fluoride (PVDF) membranes (Millipore, USA) using a semi-dry transfer apparatus (Bio-rad) at 15 mV for 1 h at room temperature. The membranes were blocked using 1 × TTBS (Tween20/Tris-buffered salt solution) containing 5% nonfat milk for 2 h at room temperature. Primary rabbit anti-ERK antibody (1:200, Santa Cruz), mouse anti-phospho-ERK antibody (1:200, Santa Cruz), mouse anti-C-myc (1:200), rabbit anti-PCNA (1:200), rabbit anti-cyclin A (1:200), rabbit anti-CDK2 (1:200), mouse anti-$p21^{CIP1}$ (1:200) and rabbit anti-β-actin antibodies were added to the blocking buffer and incubated overnight at 4 °C. Membranes were washed three times in 1 × TTBS, for 15 min each, on a shaker. The blots were then incubated with compatible mouse anti-rabbit IgG-HRP or goat anti-mouse IgG-HRP (1:2500, KPL Gaithersburg, MD) for 2 h at room temperature. The blots were washed in TTBS three times, for 15 min each. The proteins were visualised using ECL™ Western blotting detection reagents (Amersham, USA), and the signals were detected using Image Station 4000R (Kodak, USA). β-Actin was used as a protein loading control. All the experiments were performed at least twice with similar results. Quantification of the Western blot results was performed using Bandscan 5.0 software.

2.9. Plasmids, transient transfection, cell viability assay and gene expression.

The full-length ERK cDNA was isolated from the HCC cell line SMMC-7721 using PCR with the following primer pairs: 5′-AATAAGCTTCCTTCCTCCTCCTCCCGGTC-3′ (forward), 5′-GCTCTAGATTAAGATCTGTATCCTGGCTGG-3′ (reverse). The PCR product was cloned into the pCMV(+) vector (Invitrogen, NY, USA) to create the pCMV(+)-ERK plasmid. The orientation of the insert and the cDNA product were verified by sequencing. The cells were cultured in 6-well plates and transfected with pCMV(+)-ERK or a blank vector using FuGene HD reagents according to the manufacturer's instructions (Basel, Switzerland). After 36 h of transfection, the medium was replaced with DMEM supplemented with 10% (v/v) FBS.

The cells were fixed with 4% paraformaldehyde in PBS (pH 7.4), permeabilised with 0.5% Triton X-100 in PBS, and washed with PBS at room temperature. After blocking with 5% milk in PBS, the cells were incubated with the rabbit anti-ERK antibody (1:200, Santa Cruz, CA) at 4 °C for 12 h. The cells were incubated with Cruz Marker™ compatible goat anti-rabbit IgG-FITC (1:500, Santa Cruz, CA) at 37 °C for 1 h followed by three 15-min washes in PBS. Images were captured under a confocal microscope (FV500, Olympus, Japan). The effect of different treatments on cell viability was determined by the CCK-8 assay. The expression of ERK, p-ERK and C-myc was determined by Western blotting. All the experiments were performed at least twice with similar results. The results were analysed using Image-Pro Plus 6.0 or Bandscan 5.0 software.

2.10. Statistical analyses

Data were expressed as means ± SD. Statistical differences were analysed by one-way ANOVA followed by Tukey's post-hoc tests. A value of $P < 0.05$ was considered a statistically significant difference.

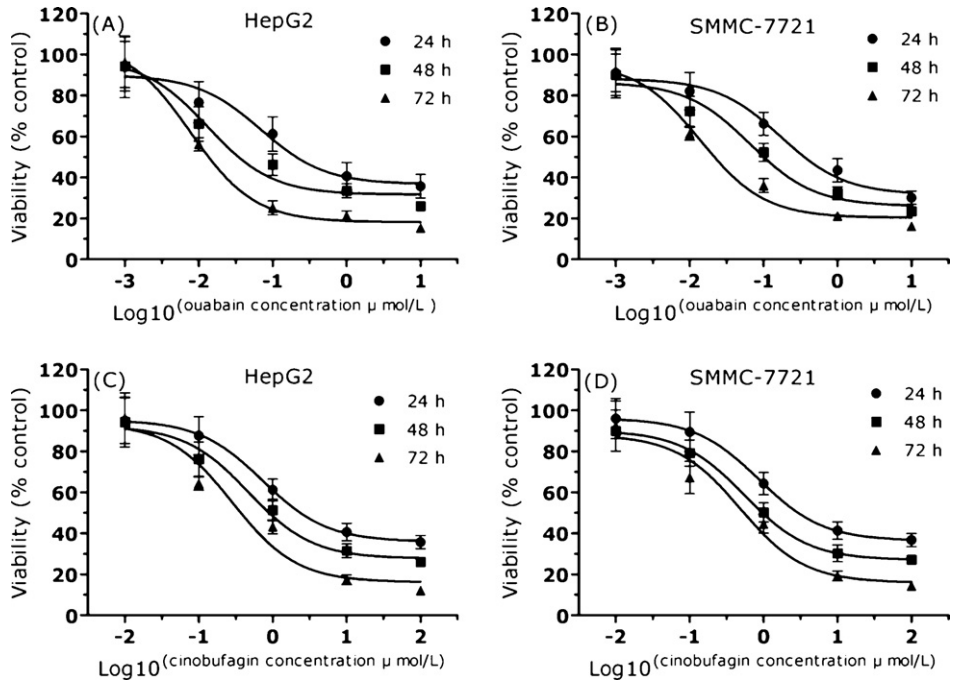

Fig. 1. Effects of ouabain and cinobufagin on the viability of HepG2 and SMMC-7721 cells. (A) and (B) Ouabain inhibited the proliferation of HepG2 or SMMC-7721 cells in time- and dose-dependent manners. (C) and (D) Cinobufagin inhibited the proliferation of HepG2 or SMMC-7721 cells in time- and dose-dependent manners. Each data point represents the mean ± standard error of three independent experiments.

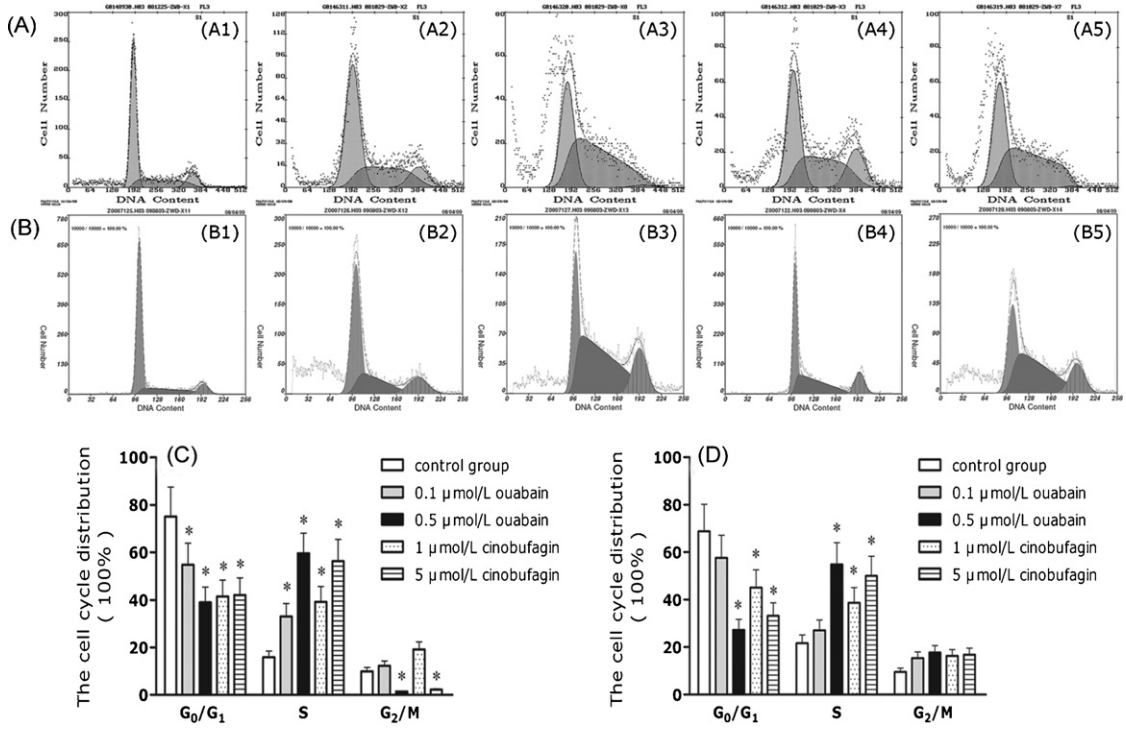

Fig. 2. Effects of ouabain and cinobufagin on cell cycle distribution in HepG2 and SMMC-7721 cells for 24 h assessed by Flow Cytometry. (A) Cell cycle distribution of HepG2 cells subjected to different treatments for 24 h (A1: control; A2: 0.1 μmol/L ouabain; A3: A2: 0.5 μmol/L ouabain; A4: 1 μmol/L cinobufagin; A5: 5 μmol/L cinobufagin). (B) Cell cycle distribution of SMMC-7721 cells subjected to different treatments (B1: control; B2: 0.1 μmol/L ouabain; B3: A2:0.5 μmol/L ouabain; B4: 1 μmol/L cinobufagin; B5: 5 μmol/L cinobufagin). (C) Columns and vertical bars represent the mean ± standard error ($n = 3$). The proportions of the 0.5 and 0.1 μmol/L ouabain and 5 and 1 μmol/L cinobufagin groups at S phase increased significantly compared with the HepG2 control group ($^*P < 0.05$). The proportions of the 0.5 and 0.1 μmol/L ouabain and 5 and 1 μmol/L cinobufagin groups at G_0/G_1 phase decreased significantly compared with the control group ($^*P < 0.05$). The proportions of the 0.5 μmol/L ouabain and 5 μmol/L cinobufagin groups at G_2/M phase decreased significantly compared with the control group ($^*P < 0.05$). (D) Columns and vertical bars represent the mean ± standard error ($n = 3$). The proportions of 0.5 μmol/L ouabain and 5 and 1 μmol/L cinobufagin groups at S phase increased significantly compared with the SMMC-7721 control group ($^*P < 0.05$).

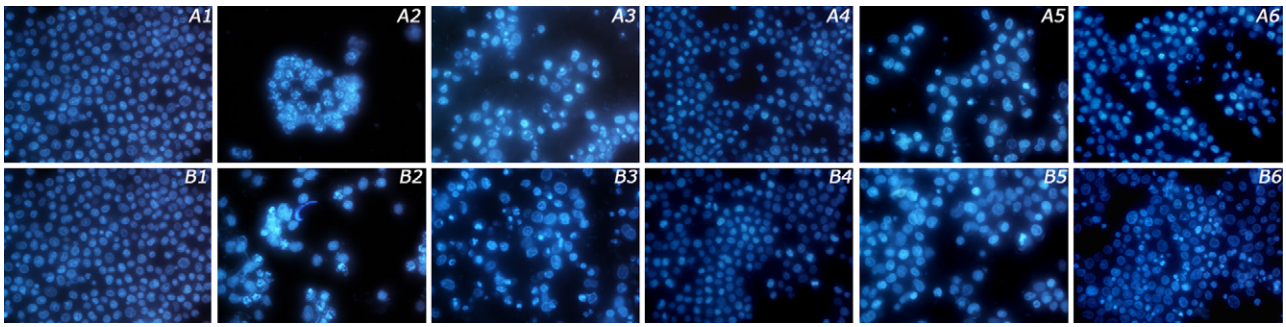

Fig. 3. Effects of ouabain and cinobufagin treatments for 24 h on the induction of apoptosis in HepG2 and SMMC-7721 cells assessed by fluorescence microscopy (200×). (A1) and (B1) HepG2 and SMMC-7721 control groups; (A2) and (B2) HepG2 and SMMC-7721 cells treated with 0.5 μmol/L ouabain; (A3) and (B3) HepG2 and SMMC-7721 cells treated with 5 μmol/L cinobufagin; (A4) and (B4) HepG2 and SMMC-7721 cells treated with 2 mmol/L EGTA; (A5) and (B5) HepG2 and SMMC-7721 cells treated with 2 mmol/L EGTA + 0.5 μmol/L ouabain (A6) and (B6) HepG2 and SMMC-7721 cells treated with 2 mmol/L EGTA + 5 μmol/L cinobufagin.

3. Results

3.1. Effects of ouabain and cinobufagin on the growth of HepG2 and SMMC-7721 cells

The CCK-8 assay was performed to analyse the effects of ouabain and cinobufagin on the viability of HepG2 and SMMC-7721 cells. As shown in Fig. 1, ouabain and cinobufagin inhibited the growth of cells in both a time- and dose-dependent manner (*$P < 0.05$). The IC_{50} values (the concentration of ouabain or cinobufagin that results in a 50% reduction in absorbance compared with the control) of cells treated for 24, 48 and 72 h were calculated based on the CCK-8 assay. The IC_{50} values for ouabain were 0.25, 0.04, and 0.01 μmol/L in HepG2 cells and 0.34, 0.11 and 0.02 μmol/L in SMMC-7721 cells at 24, 48 and 72 h, respectively. The IC_{50} values for cinobufagin were 2.82, 0.90 and 0.32 μmol/L for HepG2 cells and 3.04, 1.03 and 0.42 μmol/L for SMMC-7721 cells at 24, 48, and 72 h, respectively. These results reflected the antiproliferative effect of ouabain and cinobufagin on HepG2 and SMMC-7721 cells.

3.2. Effects of ouabain and cinobufagin on the cell cycle

The abilities of ouabain and cinobufagin to affect specific phases of the cell cycle may provide clues to explain the mechanism of action of these compounds. HepG2 and SMMC-7721 cells were exposed to 0.1 and 0.5 μmol/L ouabain and 1 and 5 μmol/L cinob-

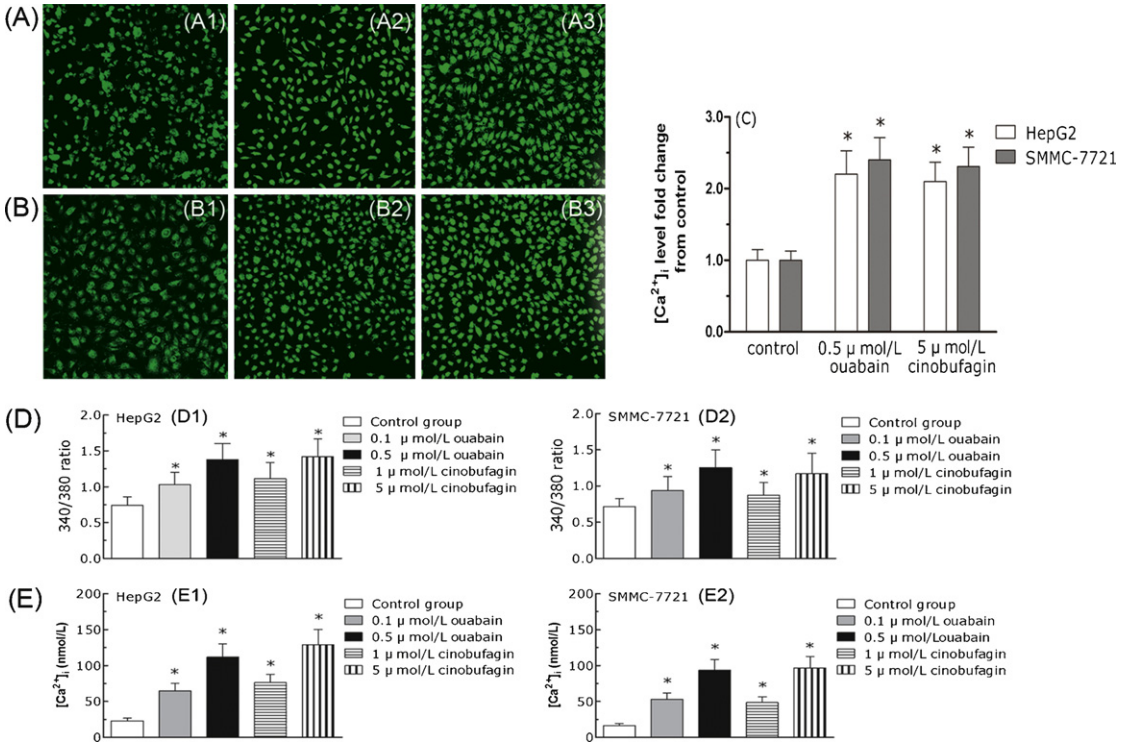

Fig. 4. Measurement of $[Ca^{2+}]_i$ in HepG2 and SMMC-7721 cells treated with ouabain or cinobufagin for 24 h by confocal microscope or spectrofluorophotometer. (A) and (B) The images of $[Ca^{2+}]_i$ loaded Fura-3/AM under different treatments were captured using a confocal microscope (100×). (A1) and (B1) The images of $[Ca^{2+}]_i$ in HepG2 and SMMC-7721 cells, respectively; (A2) and (B2) The images of $[Ca^{2+}]_i$ in HepG2 and SMMC-7721 cells, respectively, treated with 0.5 μmol/L ouabain for 24 h; (A3) and (B3) The images of $[Ca^{2+}]_i$ in HepG2 and SMMC-7721 cells, respectively, treated with 5 μmol/L cinobufagin for 24 h; (C) Columns and vertical bars represent the mean ± standard error ($n = 3$); the fura-3/AM $[Ca^{2+}]_i$ labelling of cells treated with 0.5 μmol/L ouabain and 5 μmol/L cinobufagin groups was significantly higher compared with the control group (*$P < 0.05$). (D) Measurement of the 340/380 ratio by dual-wavelength spectrofluorophotometer. (D1) and (D2) The 340/380 ratios of HepG2 or SMMC-7721 cells treated with 0.1 and 0.5 μmol/L ouabain or 1 and 5 μmol/L cinobufagin for 24 h were significantly higher than those of the control group (*$P < 0.05$). (E) The values of $[Ca^{2+}]_i$ were calculated by R_{max}, R_{min} and Sfb. Columns and vertical bars represent the mean ± standard error($n = 3$); (E1) and (E2) The $[Ca^{2+}]_i$ values of HepG2 and SMMC-7721 cells, respectively, loaded with fura-2/AM and treated with 0.5 μmol/L ouabain and 5 μmol/L cinobufagin were significantly higher than those of the control group (*$P < 0.05$).

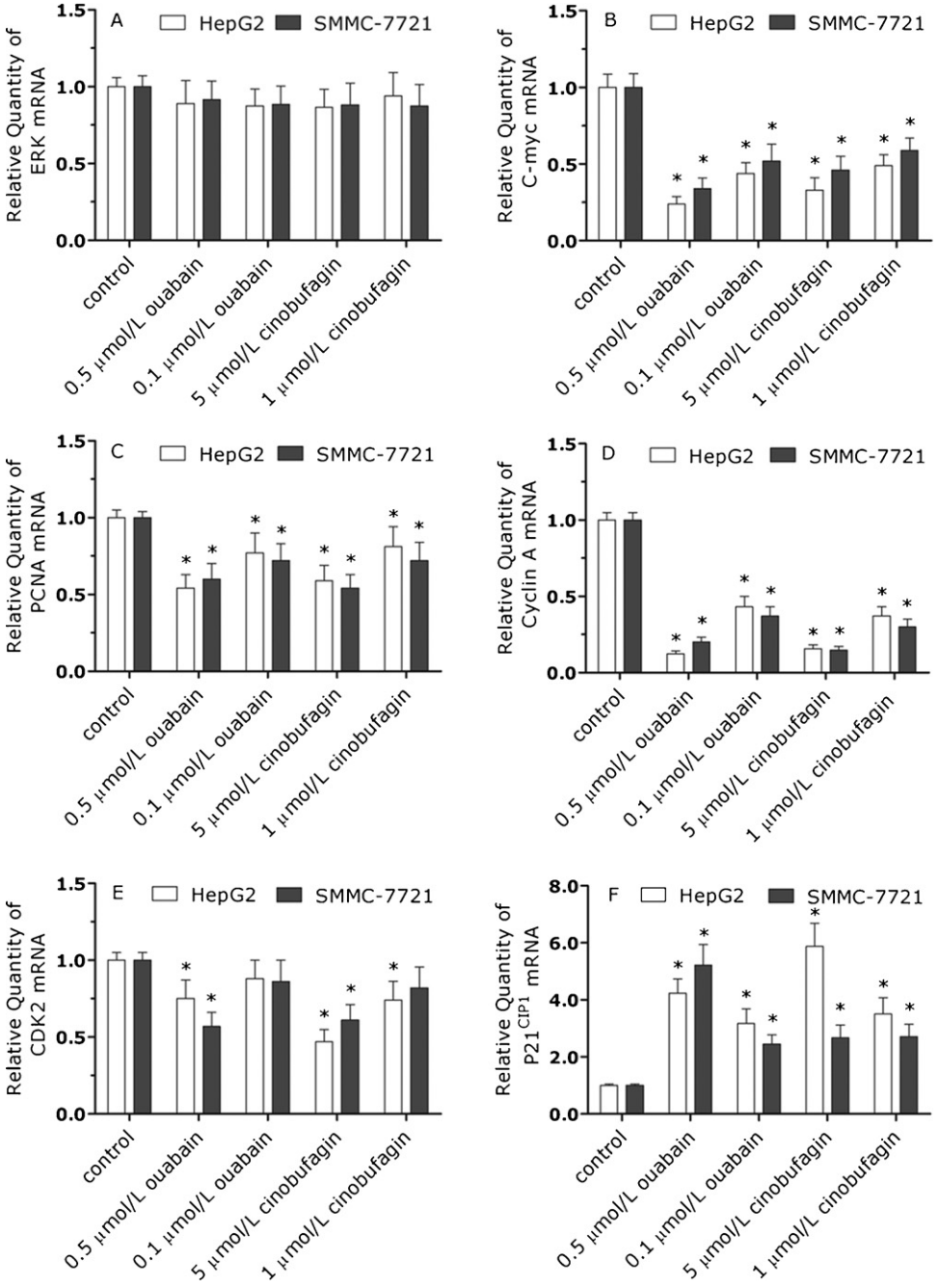

Fig. 5. Effects of ouabain and cinobufagin on the expression of ERK, C-myc, PCNA, Cyclin A, CDK2 and $P21^{CIP1}$ mRNA. HepG2 and SMMC-7721 cells were subjected to different treatments (0.5 and 0.1 μmol/L ouabain; 5 and 1 μmol/L cinobufagin) for 24 h. Total RNA was isolated and subjected to cDNA synthesis followed by real-time PCR analysis using specific primer pairs. The signals were normalised to a β-actin internal control, and the results were expressed as fold induction in comparison to control (mean ± standard error $n = 3$). *Significantly different from control, $P < 0.05$. The results of real-time PCR indicated that ouabain or cinobufagin did not affect ERK mRNA expression but down-regulated C-myc, PCNA, Cyclin A and CDK2 mRNA expression as well as *up-regulated* $P21^{CIP1}$ mRNA expression.

ufagin for 24 h. Fig. 2 shows the arrest of the cell cycle at S phase in treated cells. The proportions of HepG2 and SMMC-7721 cells in S phase were 15.8 ± 2.61% and 21.6 ± 3.52% in the control group, 33.0 ± 5.45% and 59.6 ± 8.45% and 29.5 ± 4.87% and 54.9 ± 9.06% in HepG2 and SMMC-7721 cells treated with 0.1 and 0.5 μmol/L ouabain, respectively. The proportions of HepG2 and SMMC-7721 cells in S phase were 39.2 ± 6.47% and 56.3 ± 9.12%, respectively, in cells treated with 1 μmol/L cinobufagin and 38.7 ± 6.39% and 50.0 ± 8.25%, respectively, in cells treated with 5 μmol/L cinobufagin. The proportions of cells in S phase in the ouabain or cinobufagin groups were significantly increased compared with the control group (*$P < 0.05$, $n = 3$). These results indicated that ouabain and cinobufagin might change the cell cycle distribution, in particular by increasing the proportion of cells in S phase.

3.3. *Effects of ouabain and cinobufagin on apoptosis*

As shown in Fig. 3, following exposure to 0.5 μmol/L ouabain and 5 μmol/L cinobufagin for 24 h, the cells underwent significant morphological changes. Treated cells detached from the culture plate and shrank, forming small apoptotic bodies. Other characteristic signs of apoptosis, such as nuclear condensation and fragmentation, were also observed by Hoechst 33342 staining. The proportion of apoptotic cells among those treated with

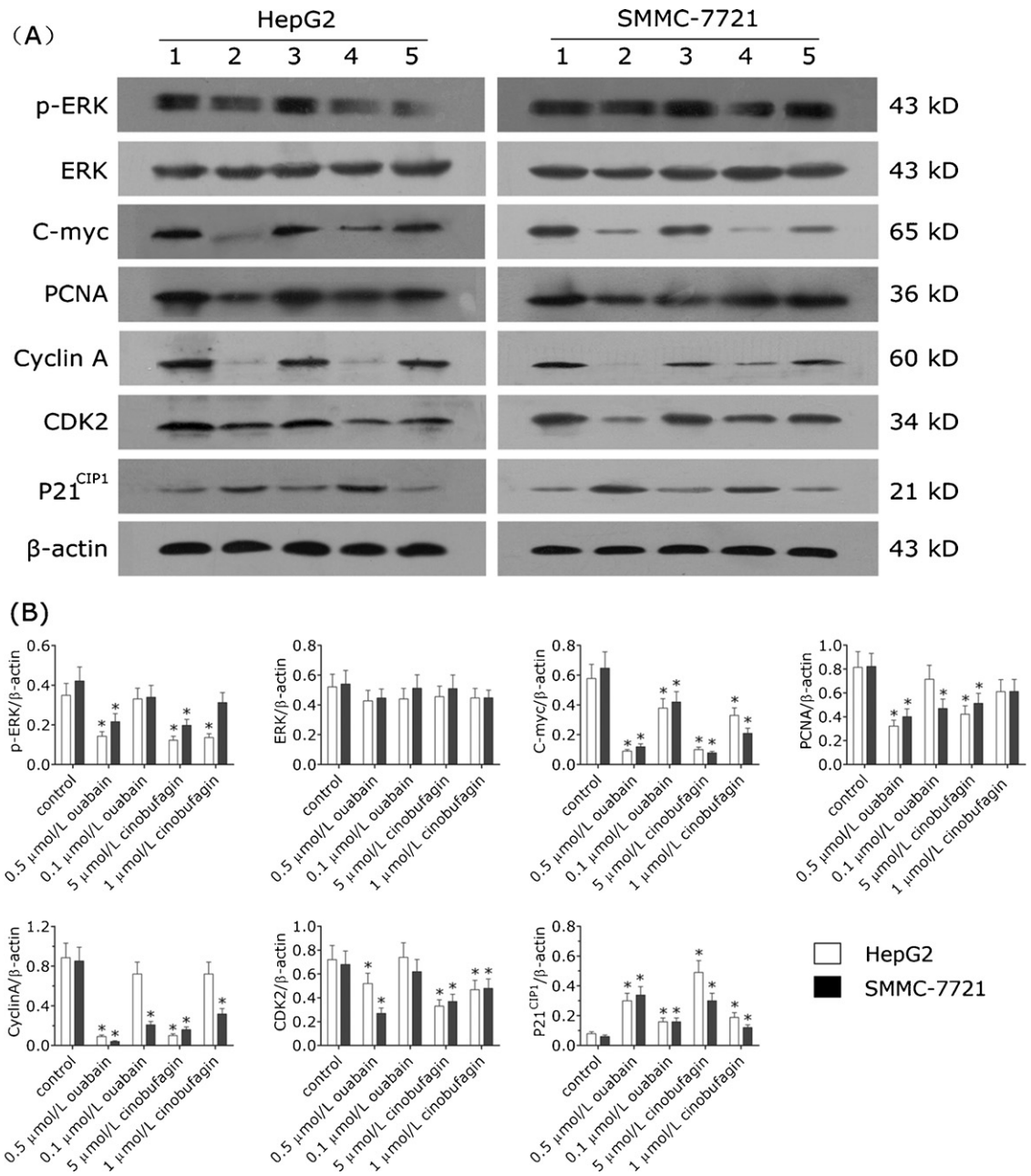

Fig. 6. Effects of ouabain and cinobufagin on the expression of ERK, C-myc, PCNA, Cyclin A, CDK2 and $P21^{CIP1}$ proteins. HepG2 and SMMC-7721 cells were incubated with different concentrations of ouabain and cinobufagin for 24 h. (A) shows the Western blot results. 1: HepG2 control group; 2: Cells treated with 0.5 μmol/L ouabain; 3: Cells treated with 0.1 μmol/L ouabain; 4: Cells treated with 5 μmol/L cinobufagin; 5: Cells were treated with 1 μmol/L cinobufagin. Western blots showing the expression of ERK, C-myc, PCNA, Cyclin A, CDK2 and $P21^{CIP1}$ are shown. β-actin was used as an internal control. Each experiment was repeated three times with similar results. Histograms represent densitometry measurement of specific bands using β-actin levels as a control. *Significantly different from control, $P < 0.05$. The results of Western blotting indicate that ouabain or cinobufagin did not affect the expression of ERK but attenuated ERK phosphorylation and down-regulated the expression of C-myc, PCNA, Cyclin A and CDK2 as well as up-regulated the expression of $P21^{CIP1}$.

2 mmol/L EGTA + 0.5 μmol/L ouabain or 5 μmol/L cinobufagin was reduced significantly compared with the 0.5 μmol/L ouabain or 5 μmol/L cinobufagin groups ($P < 0.05$). Apoptosis-related morphological alterations were not found in control or 2 mmol/L EGTA treated cells. These results indicated that ouabain and cinobufagin induced apoptosis in HepG2 and SMMC-7721 cells and that this effect was suppressed by treatment with 2 mmol/L EGTA.

3.4. Intracellular free Ca^{2+} concentration ($[Ca^{2+}]_i$)

Fig. 4A and B show $[Ca^{2+}]_i$ in HepG2 and SMMC-7721 cells through images captured by confocal microscopy. The fluorescence intensity was analysed by Image-Pro Plus 6.0 software. The $[Ca^{2+}]_i$ fluorescence intensities of the HepG2 and SMMC-7721 controls were 114.76 ± 16.84 and 94.52 ± 14.51, respectively. In HepG2 and SMMC-7721 cells treated with 0.5 μmol/L ouabain, fluorescence intensities were 252.28 ± 26.14 and 227.16 ± 23.54, respectively; in HepG2 and SMMC-7721 cells treated with 5 μmol/L cinobufagin, these values were 241.54 ± 20.12 and 218.46 ± 19.31, respectively. The $[Ca^{2+}]_i$ fluorescence intensity of HepG2 and SMMC-7721 cells treated with 0.5 μmol/L ouabain or 5 μmol/L cinobufagin was significantly increased compared with the control group (*$P < 0.05$).

Fig. 4D and E show the results of the measurement of $[Ca^{2+}]_i$ in cells treated with 0.1 and 0.5 μmol/L ouabain or 1 and 5 μmol/L

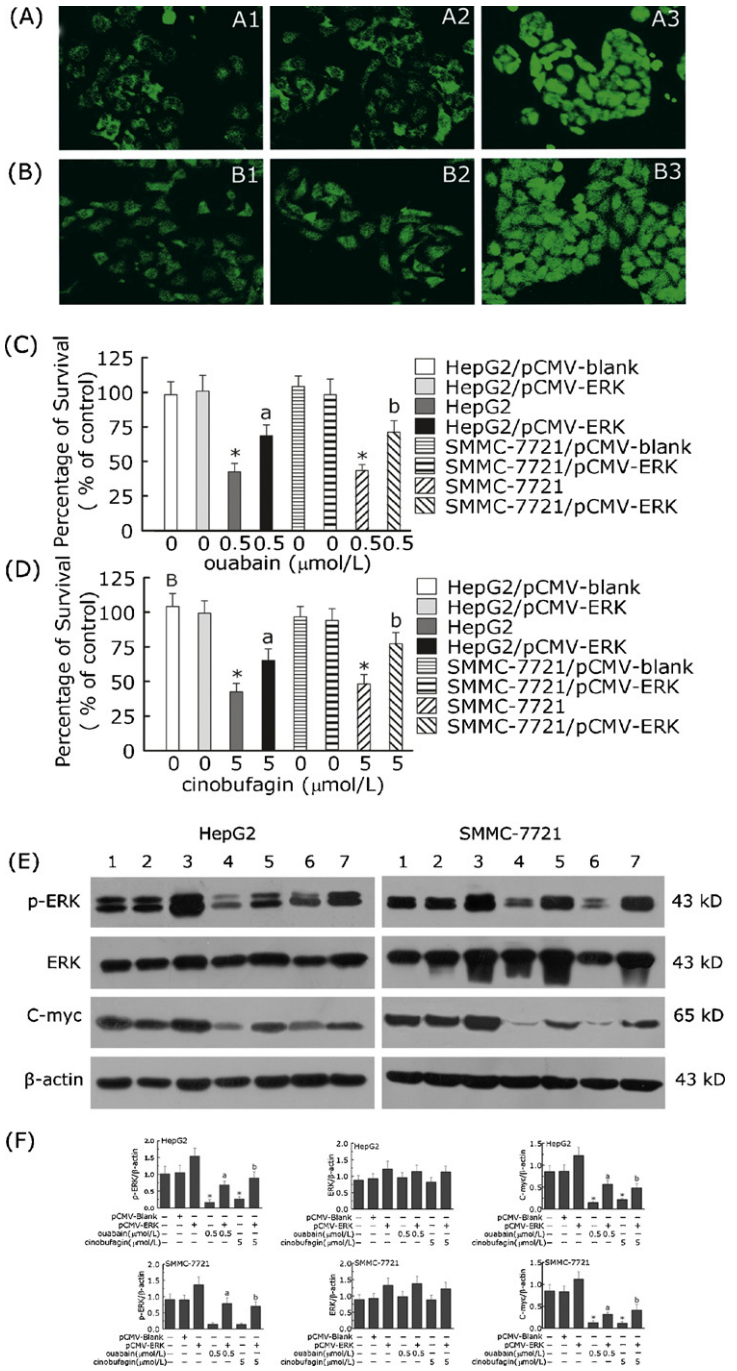

Fig. 7. The role of ERK in the antiproliferation effects induced by ouabain and cinobufagin in HepG2 and SMMC-7721 cells. (A) and (B) The expression level of ERK on cells was detected by immunocytochemistry (200×). (A1) and (B1) HepG2 and SMMC-7721 cells, respectively; (A2) and (B2) HepG2/pCMV-blank and SMMC-7721/pCMV-blank cells, respectively; (A3) and (B3) HepG2/pCMV-ERK and SMMC-7721/pCMV-ERK cells, respectively. (C) and (D) HepG2 and SMMC-7721 cell viabilities were measured by CCK-8 assay. Ouabain and cinobufagin were added to the medium after a 36-h transfection. Control value = 100%, $^{*}P < 0.05$ versus control group; $^{a}P < 0.05$, $^{b}P < 0.05$ versus HepG2 or SMMC-7721 cells treated with ouabain or cinobufagin groups. (E) The expression of ERK, p-ERK and C-myc in cells treated with 0.5 μmol/L ouabain and 5 μmol/L cinobufagin for 24 h. Each lane was loaded with 60 μg of protein. Similar results were obtained in three other experiments. 1: HepG2 or SMMC-7721 cells; 2: HepG2 or SMMC-7721 /pCMV-blank cells; 3: HepG2 or SMMC-7721/pCMV-ERK cells; 4: HepG2 or SMMC-7721 cells treated with 0.5 μmol/L ouabain; 5: HepG2 or SMMC-7721/pCMV-ERK cells treated with 0.5 μmol/L ouabain; 6: HepG2 or SMMC-7721 cells treated with 5 μmol/L cinobufagin; 7, HepG2 or SMMC-7721/pCMV-ERK cells treated with 5 μmol/L cinobufagin. (F) Histograms represent densitometry measurements of specific bands using β-actin levels as a control. $^{*}P < 0.05$ versus control group; $^{a}P < 0.05$, $^{b}P < 0.05$ versus HepG2 or SMMC-7721 cells treated with ouabain or cinobufagin. These results indicated that ouabain and cinobufagin inhibited the proliferation of HepG2 and SMMC-7721 cells by attenuating ERK phosphorylation and down-regulating the expression of the downstream transcription factor C-myc.

cinobufagin for 24 h using fura-2/AM. The 340/380 ratio in HepG2 cells was 0.74 ± 0.12; the ratios in cells treated with 0.1 and 0.5 μmol/L ouabain were 1.03 ± 0.17 and 1.38 ± 0.22, respectively. The 340/380 ratios in cells treated with 1 and 5 μmol/L cinobufagin were 1.11 ± 1.23 and 1.42 ± 0.25, respectively. The 340/380 ratio in SMMC-7721 was 0.71 ± 0.11, while the ratios in cells treated with 0.1 and 0.5 μmol/L ouabain were 0.94 ± 0.19 and 1.25 ± 0.25, respectively; the ratios with 1 and 5 μmol/L cinobufagin were 0.88 ± 0.17 and 1.17 ± 0.28, respectively. The values of $[Ca^{2+}]_i$ were calculated by R_{max}, R_{min} and Sfb. The $[Ca^{2+}]_i$ of HepG2 cells was 23.04 ± 3.80 nmol/L; the $[Ca^{2+}]_i$ for 0.1 μmol/L ouabain was 64.68 ± 10.67 nmol/L, and the $[Ca^{2+}]_i$ for 0.5 μmol/L ouabain was

111.71 ± 18.43 nmol/L. The $[Ca^{2+}]_i$ values for 1 and 5 μmol/L cinobufagin were 76.30 ± 11.45 and 128.84 ± 21.26 nmol/L, respectively. The $[Ca^{2+}]_i$ in SMMC-7721 cells was 16.67 ± 2.76 nmol/L; in cells treated with 0.1 and 0.5 μmol/L ouabain, the $[Ca^{2+}]_i$ values were 53.01 ± 8.75 and 93.36 ± 15.40 nmol/L, respectively; in cells treated with 1 and 5 μmol/L cinobufagin, these values were 48.37 ± 7.98 and 96.82 ± 15.97 nmol/L, respectively. The $[Ca^{2+}]_i$ fluorescence intensities of HepG2 and SMMC-7721 cells treated with 0.1 and 0.5 μmol/L ouabain or 1 and 5 μmol/L cinobufagin were significantly increased compared with the control group (*$P < 0.05$).The increase in $[Ca^{2+}]_i$ caused by treatment with ouabain and cinobufagin might be the cause of the apoptosis observed in these cells.

3.5. Effects of ouabain and cinobufagin on the expression levels of ERK, C-myc, cyclin A, CDK2, PCNA and $P21^{CIP1}$ mRNAs and proteins

ERK is a member of the MAPK family, which protect cells from apoptosis through the phosphorylation and activation of downstream transcription factors that regulate antiapoptotic molecules, such as C-myc, Elk1 and Bcl-XL. The C-Myc proto-oncogene is a transcription factor that has an important role in the regulation of many cellular processes, including proliferation, differentiation, cell cycle and apoptosis. The expression of C-Myc is frequently associated with tumorigenesis, autonomous proliferation and growth. The results of real-time PCR (Fig. 5A and B) and Western blotting (Fig. 6B–D) analyses indicated that 0.1 and 0.5 μmol/L ouabain and 1 and 5 μmol/L cinobufagin did not affect the expression of total ERK but attenuated ERK phosphorylation as well as down-regulated the expression of C-myc (*$P < 0.05$). Cyclin-dependent kinases (CDKs) and cyclin-dependent kinase inhibitors (CKIs) play important roles in the regulation of cell cycle. CDK2 interacts with Cyclin A and PCNA to form a complex that plays a crucial role in allowing cells to make the transition from S to G_2/M phase. $p21^{CIP1}$, which is a negative regulator of the cell cycle and inhibits CDK2 activity, is dysregulated in cancer and has been shown to directly contribute to autonomous proliferation and disruption of cellular senescence. Figs. 5 and 6 show that the expressions of PCNA (Figs. 5C and 6E), cyclin A (Figs. 5D and 6F) and CDK2 (Figs. 5E and 6G) were down-regulated compared with the control group (*$P < 0.05$), while the expression of $P21^{CIP1}$ (Figs. 5F and 6H) was up-regulated in comparison with the controls (*$P < 0.05$).

3.6. pCMV-ERK plasmid, transient transfection, cell viability assay and gene expression

In HepG2 or SMMC-7721 cells transiently transfected with the pCMV-ERK plasmid, the expression of ERK was significantly higher than in control or pCMV-blank cells ($P < 0.05$) (Fig. 7A and B). The CCK-8 assay was performed to analyse the effect of different treatments on the viability of cells. As shown in Fig. 7C and D, the survival ratio of HepG2 or SMMC-7721 cells treated with 0.5 μmol/L ouabain or 5 μmol/L cinobufagin for 24 h were 44.51 ± 6.27 and 43.41 ± 4.32%, and 42.50 ± 6.12 and 48.32 ± 6.75%, respectively. The survival rates of HepG2/pCMV-ERK or SMMC-7721/pCMV-ERK cells with the same treatments were 68.44 ± 8.10 and 71.23 ± 8.21%, and 65.21 ± 8.42 and 77.21 ± 8.21%. On the contrary, the survival ratio of pCMV-ERK or pCMV-blank group was not significantly different than the control group ($P > 0.05$). These results indicated that overexpression of ERK significantly antagonised the antiproliferation effect of ouabain or cinbufagin (*$P < 0.05$). Fig. 7E and F show that 0.5 μmol/L ouabain or 5 μmol/L cinobufagin did not affect the expression of total ERK, but attenuated ERK phosphorylation and down-regulated the expression of C-myc in HepG2 or SMMC-7721 cells (*$P < 0.05$). The expression of ERK and C-myc in HepG2/pCMV-ERK or SMMC-7721/pCMV-ERK cells treated with 0.5 μmol/L ouabain or 5 μmol/L cinobufagin was significantly higher than in HepG2 or SMMC-7721 cells subjected to the same treatments ($^bP < 0.05$). These results indicated that ouabain and cinobufagin inhibited the proliferation of HepG2 and SMMC-7721 cells by inhibiting the phosphorylation of ERK and down-regulating the expression of the downstream transcription factor C-myc.

4. Discussion

Recent studies have shown that the expression of Na^+/K^+-ATPases in mammalian cells was closely related to the incidence, development and migration of cancer and played key roles in ion transport, metabolism and signal transduction. Hence, targeting Na^+/K^+-ATPases to treat malignant tumours has become a focal point of research. Johnson et al. used cell-based high-throughput screening of chemical libraries against several potential cancer targets and found that a class of CSs potently inhibited the plasma membrane Na^+/K^+-ATPase, resulting in the inhibition of four of six prostate cancer target genes [21]. Additionally, several CSs have also shown significant antitumor activities in experimental cancer models [22–27]. The data from the present study indicated that ouabain or cinobufagin, as representative types of CSs, displayed significant anticancer activity through the inhibition of cell proliferation, induction of apoptosis and alteration of cell cycle distribution.

The receptor for CSs was the Na^+/K^+-ATPase, which represents a very interesting and potentially selective target in anticancer therapy because the expression levels of its various α and β subunits are markedly different in cancer cells compared with normal cells [6]. The signalling pathways affected by CSs are different in normal (pro-proliferative) and cancer cells (anti-proliferative). Thus, it was not surprising to find evidence of different CSs-mediated mechanisms of action in different cell types. The results of previous studies also suggested overall higher levels of the Na^+/K^+-ATPase α1 subunit in a larger proportion of clinical HCC tissue samples compared with those in normal liver tissues [28]. We concluded that the overexpression of the Na^+/K^+-ATPase would provide more binding sites for CSs on HCC cells.

The treatment with CSs reduced mortality and hospitalisation time in patients with chronic systolic and diastolic heart failure, and several CSs are endogenously produced in mammals, but a narrow therapeutic index related to their inotropic effects has hindered their development as anticancer agents. The modified CS 19-Hydroxy-2″-oxovoruscharin (coded UNBS1450) was chemically extracted from the root bark of the African plant Calotropis by means of hemi-synthesis, and UNBS1450 showed remarkable anticancer properties in different types of cancer cell lines, including non-small-cell lung cancer (A549, SW-1573), colon cancer (HCT116, S1), myelocytic leukaemia (HL-60) and breast cancer (MDA-MB-231) [9]. Mijatovic found that CSs inhibited Na^+/K^+-ATPase activity causing alterations in Na^+ and K^+ homeostasis, simultaneously down-regulating the expression of the antiapoptotic proteins Bcl-2 and Bcl-XL and inducing apoptosis [29].

However, intracellular free Ca^{2+} ($[Ca^{2+}]_i$) also plays a critical role in CSs-mediated cancer cell apoptosis. Our studies demonstrated that inhibition of Na^+/K^+-ATPase by ouabain or cinobufagin increases $[Ca^{2+}]_i$. Possible explanations for this effect are: first, inhibition of Na^+/K^+-ATPase could reduce Na^+/K^+ exchange (intracellular Na^+ for extracellular K^+), causing membrane depolarisation, activating voltage dependent Ca^{2+} channels, resulting in the influx of extracellular Ca^{2+} [30]; secondly, increased intracellular Na^+ ($[Na^+]_i$) might switch Na^+/Ca^{2+} exchanger function to the reverse mode [31]; finally, inhibiting Na^+/K^+-ATPase activity could reduce the dephosphorylation of ATP, which would

promote the phosphorylation of the Na^+/K^+-ATPase, and increase the permeability of the cell membrane to extracellular Ca^{2+} or induce the expression of Calcium-Binding Protein (CABP) [32]. $[Ca^{2+}]_i$ acts as a second messenger and is essential for the maintenance of the ionic balance and signal transduction in physiological concentrations, but a high concentration $[Ca^{2+}]_i$ can cause double-strand DNA breaks and induce apoptosis, activate Ca^{2+}/Mg^{2+} dependent nucleate endonuclease, inhibit topoisomerase I and II activities and change chromosomal structure [33,34]. As shown in Fig. 3, ouabain or cinobufagin induced typical apoptotic features of cells such as membrane blebbing, cell shrinkage and detachment, and nuclear condensation and fragmentation.

ERK is a member of the MAPK family, which protects cells from apoptosis through the phosphorylation and activation of downstream transcription factors that regulate antiapoptotic molecules, such as IAPs, TRAF1/2 and Bcl-Xl. Elevated or deregulated expression of C-Myc has been detected in a wide range of human cancers and is associated with aggressive, poorly differentiated tumours [35,36]. We found that ouabain or cinobufagin could inhibit the proliferation of HepG2 and SMMC-7721 cells. This anticancer effect was mediated by the attenuation of ERK phosphorylation correlated with the down-regulation of C-myc expression. Our data further confirmed that the expressions of p-ERK and C-myc were up-regulated by pCMV-ERK. In addition, the antiproliferation effects of CSs on HepG2 and SMMC-7721 cells were blocked by transient transfection with pCMV-ERK.

The cell cycle checkpoint control mechanism is essential for the maintenance of genome stability. An increase in $[Ca^{2+}]_i$ induced double-strand DNA breaks is one of the most important signs of cell cycle arrest. The progression through the mammalian cell cycle is regulated by the sequential activation of CDKs at specific phases of the cell cycle. The activity of CDKs is dependent on their association with cyclins, which are cofactors whose levels oscillate throughout the cell cycle. PCNA is a positive regulator of DNA synthesis that binds to the cyclin/CDK complex to regulate cell cycle progression. As cyclin levels fluctuate, the activities of associated CDKs fluctuate accordingly. Cyclins also contribute to the substrate specificity of CDKs. The negative regulator of the cell cycle $p21^{CIP1}$ inhibits the activity of the CyclinA/CDK2/PCNA complex [37–41] and plays a crucial role in the transition of cells from S to G_2/M phases. In the present study, the effects of ouabain or cinobufagin on the inhibition of HepG2 and SMMC-7721 cell proliferation were found to be associated with the induction of cell cycle arrest at the S phase through the down-regulation of the expression of Cyclin A, CDK2 and PCNA as well as the up-regulation of the expression of $P21^{CIP1}$.

The present data support the application of CSs as chemotherapy for human hepatoma chemotherapies. However, the existence of the pump in the normal liver could hinder its effectiveness as a target for therapy. Studies have shown that a low concentration of CSs promotes the proliferation of normal cells but inhibits the growth of tumour cells. There are several possible explanations for this finding: the Na^+/K^+-ATPase $\alpha 1$ of HCC cells was expressed at high levels, which results in the magnification of CS mediated intracellular signalling to inhibit tumour cell growth [28]. In addition, significant differences in intracellular acidity between tumour cells and normal cells exist. The intracellular pH is 7.12–7.65 in tumour cells, while it is 6.99–7.20 in normal cells. The alkaline environment within cancer cells plays a critical role in cell proliferation. CSs inhibit the activity of the Na^+/K^+-ATPase and activate the Na^+–H^+ exchanger, thereby changing the alkaline environment within the tumour cells to promote apoptosis [42,43]. Taken together, these findings support the feasibility of CSs as a new anticancer agent.

The present results provided evidence to support prior findings showing the anticancer effect of CSs by demonstrating the effects of these agents on inhibition of cell proliferation, induction of apoptosis and S phase cell cycle arrest in HepG2 and SMMC-7721 cells. These observations emphasised the potential usefulness of developing CSs as anticancer agents. Future studies will focus on establishing animal models to explore the anticancer activity of CSs and reduce cardiotoxicity, as well as limiting the side effects of this class of compounds.

Acknowledgements

The authors thank the Great Program of Science Foundation of Tianjin (06YFJMJC10400) and the Science Foundation of Medical College of the Chinese People's Armed Police Forces (WYM201003) for financial support of this research. This work was supported by the National Natural Science Foundation of China (No. 30840010).

References

[1] J.N. Yuan, Y. Chao, W.P. Lee, C.P. Li, R.C. Lee, F.Y. Chang, S.H. Yen, S.D. Lee, J. Whang-Peng, Chemotherapy with etoposide, doxorubicin, cisplatin, 5-fluorouracil, and leucovorin for patients with advanced hepatocellular carcinoma, Med. Oncol. 25 (2) (2008) 201–206 (PubMed:18488159).
[2] R Poupon, L. Fartoux, O. Rosmorduc, Therapeutic advances in hepatocellular carcinoma, Bull. Acad. Natl. Med. 192 (1) (2008) 23–31 (PubMed:18663979).
[3] A.Y. Bagrov, J.I. Shapiro, O.V. Fedorova, Endogenous cardiotonic steroids: physiology, pharmacology, and novel therapeutic targets, Pharmacol. Rev. 61 (1) (2009) 9–38 (PubMed:19325075).
[4] I. Prassas, E.P. Diamandis, Novel therapeutic applications of cardiac glycosides, Nat. Rev. Drug Discov. 7 (11) (2008) 926–935 (PubMed:18948999).
[5] T. Mijatovic, E. Van Quaquebeke, B. Delest, O. Debeir, F. Darro, R. Kiss, Cardiotonic steroids on the road to anti-cancer therapy, Biochim. Biophys. Acta 1776 (1) (2007) 32–57 (PubMed:17706876).
[6] T. Mijatovic, L. Ingrassia, V. Facchini, R. Kiss, Na^+/K^+-ATPase alpha subunits as new targets in anticancer therapy, Expert Opin. Ther. Targets 12 (11) (2008) 1403–1417 (PubMed:18851696).
[7] B. Stenkvist, Cardenolides cancer, Anticancer Drugs 12 (7) (2001) 635–638 (PubMed:11487722).
[8] T. Mekhail, H. Kaur, R. Ganapathi, G.T. Budd, P. Elson, R.M. Bukowski, Phase 1 trial of Anvirzel in patients with refractory solid tumors, Invest. New Drugs 24 (5) (2006) 423–427 (PubMed:16763787).
[9] T. Mijatovic, U. Jungwirth, P. Heffeter, M.A. Hoda, R. Dornetshuber, R. Kiss, W. Berger, The Na^+/K^+-ATPase is the Achilles heel of multi-drug-resistant cancer cells, Cancer Lett. 282 (1) (2009) 30–34 (PubMed:19339106).
[10] J.A. Smith, T. Madden, M. Vijjeswarapu, R.A. Newman, Inhibition of export of fibroblast growth factor-2 (FGF-2) from the prostate cancer cell lines PC3 and DU145 by Anvirzel and its cardiac glycoside component, oleandrin, Biochem. Pharmacol. 62 (4) (2001) 469–472 (PubMed:11448457).
[11] T. Mijatovic, N. De Nève, P. Gailly, V. Mathieu, B. Haibe-Kains, G. Bontempi, J. Lapeira, C. Decaestecker, V. Facchini, R. Kiss, Nucleolus and c-Myc: potential targets of cardenolide-mediated antitumor activity, Mol. Cancer Ther. 7 (5) (2008) 1285–1296 (PubMed:18483316).
[12] P. Yang, D.G. Menter, C. Cartwright, D. Chan, S. Dixon, M. Suraokar, G. Mendoza, N. Llansa, R.A. Newman, Oleandrin-mediated inhibition of human tumor cell proliferation: importance of Na^+,K^+-ATPase alpha subunits as drug targets, Mol. Cancer Ther. 8 (8) (2009) 2319–2328 (PubMed:19671733).
[13] T. Mijatovic, I. Roland, E. Van Quaquebeke, B. Nilsson, A. Mathieu, F. Van Vynckt, F. Darro, G. Blanco, V. Facchini, R. Kiss, The alpha1 subunit of the sodium pump could represent a novel target to combat non-small cell lung cancers, J. Pathol. 212 (2) (2007) 170–179 (PubMed:17471453).
[14] F. Lefranc, R. Kiss, The sodium pump alpha1 subunit as a potential target to combat apoptosis-resistant glioblastomas, Neoplasia 10 (3) (2008) 198–206 (PubMed:18323016).
[15] K. Winnicka, K. Bielawski, A. Bielawska, A. Surazyński, Antiproliferative activity of derivatives of ouabain, digoxin and proscillaridin A in human MCF-7 and MDA-MB-231 breast cancer cells, Biol. Pharm. Bull. 31 (6) (2008) 1131–1140 (PubMed:18520043).
[16] L. Zhang, Z. Zhang, H. Guo, Y. Wang, Na^+/K^+-ATPase-mediated signal transduction and Na^+/K^+-ATPase regulation, Fundam. Clin. Pharmacol. 22 (6) (2008) 615–621 (PubMed:19049666).
[17] L.D. Faller, Mechanistic studies of sodium pump, Arch. Biochem. Biophys. 476 (1) (2008) 12–21 (PubMed:18558080).
[18] Z. Li, Z. Xie, The Na/K-ATPase/Src complex and cardiotonic steroid-activated protein kinase cascades, Pflug. Arch. 457 (3) (2009) 635–644 (PubMed:18283487).
[19] Y. Takada, K. Matsuo, H. Ogura, L. Bai, A. Toki, L. Wang, M. Ando, T. Kataoka, Odoroside A and ouabain inhibit Na^+/K^+-ATPase and prevent NF-kappaB-inducible protein expression by blocking Na^+-dependent amino acid transport, Biochem. Pharmacol. 78 (9) (2009) 1157–1166 (PubMed:19559678).
[20] F. Lefranc, T. Mijatovic, Y. Kondo, S. Sauvage, I. Roland, O. Debeir, D. Krstic, V. Vasic, P. Gailly, S. Kondo, G. Blanco, R. Kiss, Targeting the $\alpha 1$ subunit of sodium pump to combat glioblastoma cells, Neurosurgery 62 (1) (2008) 211–221 (PubMed:18300910).

[21] P.H. Johnson, R.P. Walker, S.W. Jones, K. Stephens, J. Meurer, D.A. Zajchowski, M.M. Luke, F. Eeckman, Y. Tan, L. Wong, G. Parry, T.K. Morgan Jr., M.A. McCarrick, J. Monforte, Multiplex gene expression analysis for high-throughput drug discovery: screening and analysis of compounds affecting genes overexpressed in cancer cells, Mol. Cancer Ther. 1 (14) (2002) 1293–1304 (PubMed:12516962).
[22] D.J. McConkey, Y. Lin, L.K. Nutt, H.Z. Ozel, R.A. Newman, Cardiac glycosides stimulate Ca^{2+} increases and apoptosis in androgen-independent, metastatic human prostate adenocarcinoma cells, Cancer Res. 60 (14) (2000) 3807–3812 (PubMed:10919654).
[23] H. Zhang, D.Z. Qian, Y.S. Tan, K. Lee, P. Gao, Y.R. Ren, S. Rey, H. Hammers, D. Chang, R. Pili, C.V. Dang, J.O. Liu, G.L. Semenza, Digoxin and other cardiac glycosides inhibit HIF-1alpha synthesis and block tumor growth, Proc. Natl. Acad. Sci. U. S. A. 105 (50) (2008) 19579–19586 (PubMed:19020076).
[24] C. Riganti, I. Campia, M. Polimeni, G. Pescarmona, D. Ghigo, A. Bosia, Digoxin and ouabain induce P-glycoprotein by activating calmodulin kinase II and hypoxia-inducible factor-1alpha in human colon cancer cells, Toxicol. Appl. Pharmacol. 240 (3) (2009) 385–392 (PubMed:19647009).
[25] A. Kassardjian, S.I. Kreydiyyeh, JNK modulates the effect of caspases and NF-kappaB in the TNF-alpha-induced down-regulation of Na^+/K^+ATPase in HepG2 cells, J. Cell. Physiol. 216 (3) (2008) 615–620 (PubMed:18348163).
[26] C.D. Simpson, I.A. Mawji, K. Anyiwe, M.A. Williams, X. Wang, A.L. Venugopal, M. Gronda, R. Hurren, S. Cheng, S. Serra, R. Beheshti Zavareh, A. Datti, J.L. Wrana, S. Ezzat, A.D. Schimmer, Inhibition of the sodium potassium adenosine triphosphatase pump sensitizes cancer cells to anoikis and prevents distant tumor formation, Cancer Res. 69 (7) (2009) 2739–2747 (PubMed:19293189).
[27] Z. Wang, M. Zheng, Z. Li, R. Li, L. Jia, X. Xiong, N. Southall, S. Wang, M. Xia, C.P. Austin, W. Zheng, Z. Xie, Y. Sun, Cardiac glycosides inhibit p53 synthesis by a mechanism relieved by Src or MAPK inhibition, Cancer Res. 69 (16) (2009) 6556–6564 (PubMed:19679550).
[28] Z.W. Xu, F.M. Wang, M.J. Gao, X.Y. Chen, W.L. Hu, R.C. Xu, Targeting the Na(+)/K(+)-ATPase alpha1 subunit of hepatoma HepG2 cell line to induce apoptosis and cell cycle arresting, Biol. Pharm. Bull. 33 (5) (2010) 743–751 (PubMed:20460749).
[29] X. Lei, Y. Chen, G. Du, W. Yu, X. Wang, H. Qu, B. Xia, H. He, J. Mao, W. Zong, X. Liao, M. Mehrpour, X. Hao, Q. Chen, Gossypol induces Bax/Bak-independent activation of apoptosis and cytochrome c release via a conformational change in Bcl-2, FASEB J. 20 (12) (2006) 2147–2149 (PubMed:16935937).
[30] X. Deng, F. Yin, X. Lu, B. Cai, W. Yin, The apoptotic effect of brucine from the seed of Strychnos nux-vomica on human hepatoma cells is mediated via Bcl-2 and Ca^{2+} involved mitochondrial pathway, Toxicol. Sci. 91 (1) (2006) 59–69 (PubMed:16443926).
[31] J. Wang, X.Q. Zhang, B.A. Ahlers, L.L. Carl, J. Song, L.I. Rothblum, R.C. Stahl, D.J. Carey, J.Y. Cheung, Cytoplasmic tail of phospholemman interacts with the intracellular loop of the cardiac Na^+/Ca^{2+} exchanger, J. Biol. Chem. 281 (42) (2006) 32004–32014 (PubMed:16921169).
[32] H.L. Roderick, S.J. Cook, Ca^{2+} signalling checkpoints in cancer: remodeling Ca^{2+} for cancer cell proliferation and survival, Nat. Rev. Cancer 8 (5) (2008) 361–375 (PubMed:18432251).
[33] R. Rizzuto, T. Pozzan, Microdomains of intracellular Ca^{2+}: molecular determinants and functional consequences, Physiol. Rev. 86 (1) (2006) 369–408 (PubMed:16371601).
[34] P. Pinton, C. Giorgi, R. Siviero, E. Zecchini, R. Rizzuto, Calcium apoptosis: ER-mitochondria Ca^{2+} transfer in the control of apoptosis, Oncogene 27 (50) (2008) 6407–6418 (PubMed:18955969).
[35] N. Meyer, L.Z. Penn, Reflecting on 25 years with MYC, Nat. Rev. Cancer 8 (12) (2008) 976–990 (PubMed:19029958).
[36] T.A. Brooks, L.H. Hurley, The role of supercoiling in transcriptional control of MYC and its importance in molecular therapeutics, Nat. Rev. Cancer 12 (2009) 849–861 (PubMed:19907434).
[37] L.W. Wheeler, N.H. Lents, J.J. Baldassare, Cyclin, A-CDK activity during G1 phase impairs MCM chromatin loading and inhibits DNA synthesis in mammalian cells, Cell Cycle 7 (14) (2008) 2179–2188.
[38] R.A. Frum, P.D. Chastain, P. Qu, S.M. Cohen, D.G. Kaufman, DNA replication in early S phase pauses near newly activated origins, Cell Cycle 7 (10) (2008) 1440–1448 (PubMed:18635963).
[39] L.F. Qin, I.O. Ng, S.T. Fan, Ng M, p21/WAF1, p53 and PCNA expression and p53 mutation status in hepatocellular carcinoma\, Int. J. Cancer 79 (4) (1998) 424–428 (PubMed:9699537).
[40] S. Diederichs, N. Bäumer, P. Ji, S.K. Metzelder, G.E. Idos, T. Cauvet, W. Wang, M. Möller, S. Pierschalski, J. Gromoll, M.G. Schrader, H.P. Koeffler, W.E. Berdel, H. Serve, C. Müller-Tidow, Identification of interaction partners and substrates of the cyclin A1-CDK2 complex, J. Biol. Chem. 279 (32) (2004) 33727–33741 (PubMed:15159402).
[41] P. Ji, S. Agrawal, S. Diederichs, N. Bäumer, A. Becker, T. Cauvet, S. Kowski, C. Beger, K. Welte, W.E. Berdel, H. Serve, C. Müller-Tidow, Cyclin A1, the alternative A-type cyclin, contributes to G1/S cell cycle progression in somatic cells, Oncogene 24 (16) (2005) 2739–2744 (PubMed:15829981).
[42] S. Matsuyama, J. Llopis, Q.L. Deveraux, R.Y. Tsien, J.C. Reed, Changes in intramitochondrial and cytosolic pH: early events that modulate caspase activation during apoptosis, Nat. Cell Biol. 2 (6) (2000) 318–325 (PubMed:10854321).
[43] R.A. Cardone, V. Casavola, S.J. Reshkin, The role of disturbed pH dynamics and the Na^+/H^+ exchanger in metastasis, Nat. Rev. Cancer 5 (10) (2005) 786–795 (PubMed:16175178).